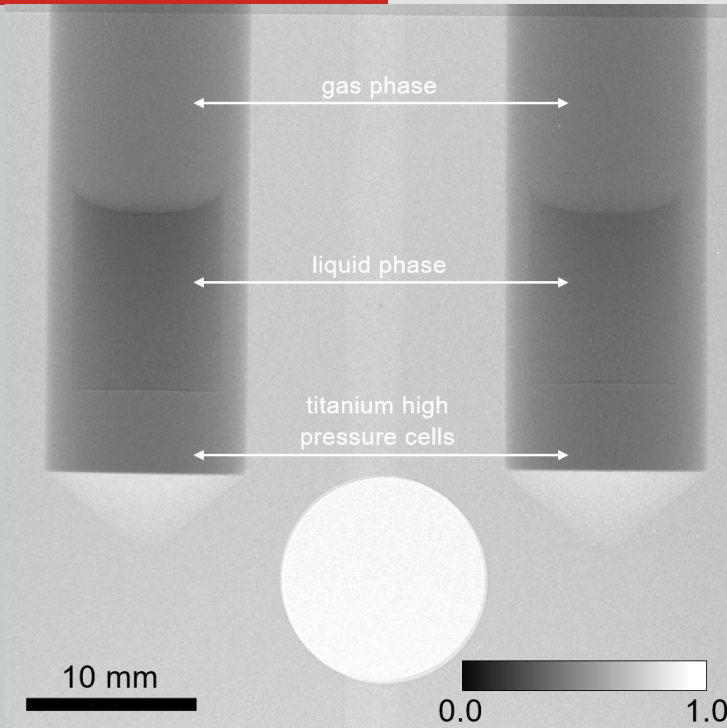


# SWISS NEUTRON NEWS



Schweizerische Gesellschaft für Neutronenforschung  
Société Suisse de la Science Neutronique  
Swiss Neutron Science Society



### **On the cover**

Neutron radiography of two vessels with still liquids under controlled external gas pressure and temperature after being pressurized with  $\text{CH}_4$  from 1.0 to 81.4 bar at 7.0 °C. The left cell contains  $n\text{-C}_{10}\text{D}_{22}$ , the right cell contains  $\text{C}_2\text{D}_6\text{O}$ .” by O. Vopička, P. Číhal, M. Klepić, J. Crha, V. Hynek, K. Trtík, P. Boillat, P. Trtik.

# Contents

- 4** The President's Page
- 6** New board member and editor of Swiss Neutron News
- 7** Data Analysis of CAMEA-like Instruments
- 15** Measurement of liquids surface tension in extreme environments using neutron imaging
- 25** Minutes of the SGN/SSN/SNSS General Assembly 2021
- 32** Announcements
- 34** Conferences and Workshops
- 39** Editorial

# The President's Page



Dear fellow neutron scientists,

Let me start by expressing my gratitude to the past president of the Swiss Neutron Science Society, Henrik Rønnow, and the former secretary, Urs Gasser, for many years of service to the Swiss neutron community since 2009. Among many other things Urs has continuously made sure that Swiss Neutron News reported on exciting neutron science developments, for example, most recently about the successful upgrade of the guide system of the Swiss spallation source, SINQ. Henrik

has done fantastic work benefitting neutron science beyond Switzerland. During his tenure, strong Swiss engagement in the upcoming European Spallation Source (ESS) was secured while Swiss membership at the Institute Laue Langevin continues. Going forward, Henrik will continue this work as the chairman of the European Neutron Scattering Association (ENSA).

This brings me to introducing changes concerning the board of our society addressing the increasing importance of neutron science. Following the philosophy of the deci-

sion in 2018 to change the name of our society to “Swiss Neutron Science Society” to reflect the openness for all researchers using neutrons, in November 2022 the general assembly unanimously decided to increase the number of SNSS board members from four to five. As a result, we welcome Florian Piegsa (University of Bern) as new board member. It was further agreed that the duties of secretary are distributed among the board members and Efthymios Polatidis (PSI) will edit Swiss Neutron News. All new board members are briefly introduced on page 6. Finally, I am thankful for all previous members for staying on the board so that we can continue to benefit from their expertise.

Aside from these important changes, it was very pleasant that we were able to have the general assembly in person including the traditional apéro. Currently, it looks like at least for this coming spring and summer we can be optimistic about many more meetings, conferences and workshops taking place in person. One such meeting that you want to keep in your calendar is a special session entitled “Swiss Neutron Science on the European Scale”, which SNSS is organizing at the annual meeting of the Swiss Physical Society, June 27 – 30, 2022 in Fribourg (<https://www.sps.ch/en/events/sps-annual-meeting-2022>). We are looking forward to

receiving your contributions and to have many in-person discussions at the meeting.

Two of such exciting examples of neutron research can also be found in this issue of Swiss Neutron News. Jakob Lass et al. report on Data Analysis of CAMEA-like Instruments and Vopička et al. on Measurement of liquids surface tension in extreme environments using neutron imaging.

I would like to close by saying that Swiss neutron scattering is entering an exciting period. The Swiss contributions to the ESS are slowly taking shape as more and more components for BIFROST, ESTIA and ODIN are currently being installed at ESS. At the Swiss ultracold neutron source (UCN), the upgraded n2EDM experiment is getting prepared for the next leading search for the neutron electric dipole moment. SINQ remains tremendously productive, is receiving further instrument upgrades, and has recently seen a nearly twofold increase in user demand. This high demand highlights the importance of the vision for neutron science in Switzerland that was summarized last year in the Swiss Neutron Science Roadmap [1].

I wish all of you an exciting year with many on-site experiments and in-person meetings.

Marc Janoschek

[1] Rønnow, HM, Gasser, U, Krämer, K, Strobl, M, & Kenzelmann, M. (2021). Neutron Science Roadmap for Research Infrastructures 2025–2028 by the Swiss Neutron Science Community. In Swiss Academies Reports (Vol. 16, Number 7). <https://doi.org/10.5281/zenodo.4637661>

# New board member and editor of Swiss Neutron News



Efthymios Polatidis

...studied mechanical engineering at the University of Thessaly (Greece, 2007) and received his doctorate by the University of Manchester (2012). Following subsequent positions as postdoctoral researcher at the Max Planck Institute for Intelligent systems, Stuttgart (2013-2016) and Photon Science Division at the Paul Scherrer Institute (2016-2018), he is tenured instrument scientist of the neutron diffraction instrument POLDI. He is responsible for the ongoing upgrade program of POLDI, as well as scientific programs related to additive manufacturing and engineering diffraction.



Florian Piegsa

...studied physics at TU Munich (Germany, 2004) and received his doctorates by the Paul Scherrer Institute and TU Munich (2009). Following subsequent positions as beamline scientist (PF2) at the Institut Laue-Langevin in Grenoble (France), as post-doc and later as senior staff scientist at ETH Zurich, he received a SNSF-Professorship and an ERC Starting Grant (2016). He was appointed to full-professor for Low Energy and Precision Physics at the University of Bern in 2021.

# Data Analysis of CAMEA-like Instruments

**J. Lass** <sup>1,2</sup>

<sup>1</sup>Nanoscience Center, Niels Bohr Institute, University of Copenhagen, DK-2100 Copenhagen Ø, Denmark

<sup>2</sup>Laboratory for Neutron Scattering and Imaging, Paul Scherrer Institute, CH-5232 Villigen, Switzerland

(Dated: March 24, 2022)

Novel multiplexing triple-axis neutron scattering spectrometers enable a simultaneous detection of scattered neutrons at various angles and energies. The significant improvement in the data acquisition rate requires a novel software package, handling the associated enhancement in data complexity. MJOLNIR is a Python-based software package that allows users to reduce, visualise and treat observables measured on various multiplexing triple-axis spectrometers at different facilities. MJOLNIR offers a user-friendly interface facilitating the implementation of additional features, such as fitting routines, modelling of multi-dimensional data or advanced machine learning algorithms. Profiting from strong collaborations within the multiplexing triple-axis community, MJOLNIR is expected to enable cutting edge research within the condensed matter research.

## I. Introduction

The understanding of novel quantum phenomena often require a thorough investigation of their microscopic interactions. Specific terms of the defining Hamiltonian are encoded in the dynamic response function  $S(\vec{Q}, \omega)$ , which can be accessed directly using inelastic neutron scattering spectroscopy. Here  $\vec{Q}$  denotes the wavevector and  $\hbar\omega = E$  the energy transfer of the neutron, respectively. The workhorse of inelastic neutron scattering dynamics is the triple axis spectrometer, where a monochromatic neutron beam is scattered by the sample and reaches a single detector via scattering from an analyser. TAS cover a single  $(\vec{Q}, E)$  point per acquisition, which is deduced directly from the specific motor positions of the instrument<sup>1</sup>. Thus, during experiments the instrument covers isolated trajectories that are mapped along  $\vec{Q}$  or  $E$  (see Fig. 1) or external parameters.

TAS can only collect neutrons that enter the detector after scattering from the analyser unit. Instruments that are equipped with several analyser-detector pairs are known as multiplexing triple-axis spectrometers. An early example of multiplexing TAS is the RITA-II instrument<sup>2</sup> at the Paul Scherrer Institute (PSI), Switzerland, where 9 individual analysers scatter the neutrons towards a 2D detector. Because of the 9 analysers, the instrument enables a simultaneous measurement of 9 individual  $(\vec{Q}, E)$  points at constant  $E$  per acquisition time (see Fig. 1). The latest development of this concept is the UFO design<sup>3</sup> at the Institut Laue-Langevin (ILL), Grenoble France, where each analyser, in addition to being rotationally motorised,

is mounted on a translation stage also allowing for small variations in  $E$ .

The measurement efficiency of multiplexing instruments can be improved by adding further analyser-detector units. Engineering constraints have shown that it is favourable to modify the instrument design for such cases. In modern multiplexing TAS, such as FlatCone<sup>5</sup> at the ILL, the analyser units are built such that they scatter the neutrons out of the horizontal scattering plane. The detectors are mounted above the analyser units allowing for a radially distributed analyser-detector pair geometry, where sizeable fractions of reciprocal space at constant  $E$  can be measured in a single sample rotation scan (see Fig. 1). The FlatCone spectrometer, for instance, employs 31 analyser-detector pairs covering a scattering angle of  $75^\circ$ . Cross-talk shielding between each pair reduces parasitic signals, but adds the requirement that for a continuous  $Q$  coverage at least two measurements with slightly shifted scattering angles are needed.

A high neutron transmission of graphite allows the mounting of several analyser units in series, enabling a simultaneous measurement of several energy transfers  $E$  at a the same scattering angle. The first instrument employing this design was Multi-FLEXX<sup>6</sup> at the Helmholtz Zentrum Berlin (HZB), Germany, using 155 single detectors distributed over 31 wedges with 5 analysers each. Thus, 5 energy slices are measured simultaneously (see Fig. 1).

The CAMEA<sup>7</sup> design at PSI is the latest step in the evolution of multiplexing TAS instruments. Here position-sensitive detectors are mounted radially above the entire analyser array providing a better spatial cov-

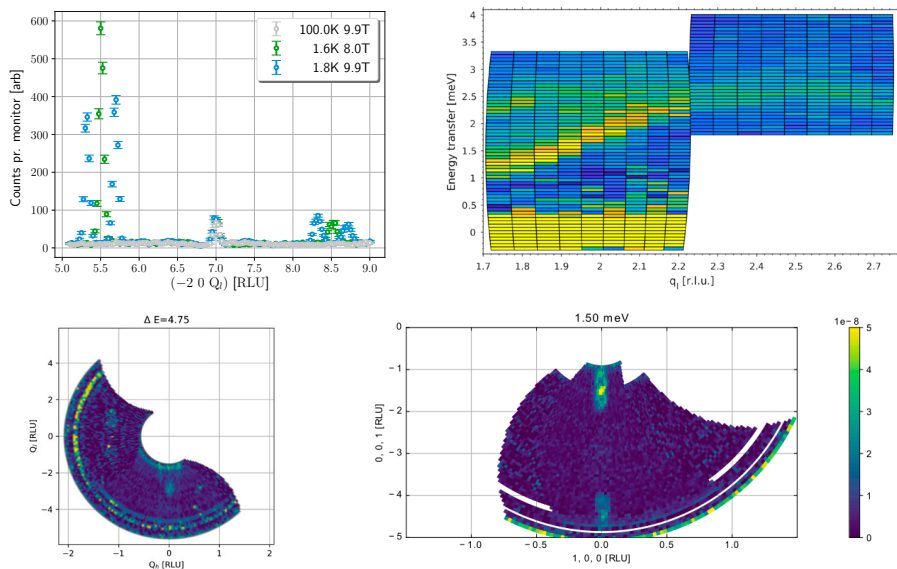


**Figure 1**

The data are taken on a single crystal of multiferroic  $\text{Ni}_3\text{TeO}_6^4$ . **Top Left:** Isolated trajectories measured on the TAS EIGER, PSI along  $(-2, 0, q)$  at  $\Delta E = 0$  meV. **Top Right:** Intensity map obtained from RITA II using two different instrumental settings to probe different energy transfer ranges between  $-0.2$  and  $4$  meV. **Bottom Left:** Constant energy plane measured with a single FlatCone, ILL setting, rotating the sample around the  $(0, k, 0)$  axis, i.e. having  $(h, 0, l)$  in the plane, at an energy transfer  $E=4.75$  meV. **Bottom Right:** 1 of 5 constant energy planes measured on MultiFLEX, HZB using 4 different instrument settings in the  $(h, 0, l)$  plane at an energy transfer  $E=1.5$  meV.

erage, and allows a discrimination between neutrons that are scattered from different analysers. At CAMEA 104 position-sensitive detector tubes are distributed over 8 wedges each consisting of 8 analysers in total covering  $60^\circ$  scattering angle. The so-called prismatic concept<sup>8</sup>, enables a subdivision of each E to establish a quasi-continuous energy coverage.

## II. Software MJOLNIR

Modern multiplexing TAS allow to measure large fractions of  $S(\vec{Q}, \omega)$  in a single sample rotation scan. Thus, while the instrument design has simplified the way experiments are performed, the post procession of data has increased significantly in complexity. The software package MJOLNIR<sup>9</sup> is designed to treat data from every multiplexing triple-axis neutron spectrometer. It offers tools to

quickly convert data from detector counts in the instrumental geometry to reciprocal space, and to interactively visualise the data in 1, 2 and 3 dimensions. The software has been written with focus on being user-friendly, offering a scripting, a command line, and a graphical interface with an intuitive transition between the three. It also works on the users computers without the need for internet access or log-in credentials.

Figure 2 showcases the main specifications upon which MJOLNIR was built. As indi-

cated on the top right, any software must aim towards being 'easy to use', which in this case is interpreted as being cross-platform compatible and written in a high-level language. As such the software is written in pure Python and is radially distributed through Python's package interface (PyPI), following the trend for academic software shifting towards Python as the standard programming language. Python is licence-free and many major packages run across all major computer platforms.



**Figure 2**

Software requirements for multiplexing instruments as implemented in MJOLNIR.

A sustainable software needs to work reliably across all computer platforms and Python versions. This is ensured through automatic testing frameworks. New software versions undergo unit and integration tests, followed by a coverage test flagging any parts of the code that was not checked. The software is checked across all major operating systems, and installation alongside compatibility tests are performed regularly. The testing scheme is also extended to the online tutorials which are adapted automatically if necessary. The software code is also documented on multiple levels. As such the source code reveals detailed notes, every function possesses callable signatures, the tutorials provide detail descriptions on how the package can be used and a list of frequently asked questions help with eventual difficulties. We also maintain an email account (MJOLNIRPackage@gmail.com) where software users can reach out directly.

Lastly, the software needs to possess a user interface. MJOLNIR offers a scripting interface, where the package is imported directly and where its functionalities can be called within regular Python scripts. While most of the online tutorials are intended for this interface, two additional interfaces are available. A command line interface offers a rudimentary visualisation option via a single line of code, and a more modern graphical user interface (GUI) has been programmed for less proficient Python users. The GUI is distributed either through a secondary python package (MJOLNIRGui) using Pip or via standard installers that are available for Windows, MacOS, and Linux (Debian). The GUI offers many MJOLNIR functionalities and allows to export converted data which can be

further processed with analysis program of choice by the user. It is also possible to directly export Python scripts which generate identical data treatment and figures as performed in the GUI. This allows to generate tutorials that are based on specific data, and includes loading, conversion, background subtraction, masking, and visualisation tools. This option often serves as the starting point for advanced data treatment in the scripting interface.

One of the main benefits of MJOLNIR is that the statistical approach appropriate for neutron scattering<sup>11</sup>, various tools for spurion detection, masking, absolute normalisation and interfacing tools with other analysis software are implemented at one central place providing uniform functionality across all instruments utilising MJOLNIR.

### III. MJOLNIR Main features

The specific tasks for MJOLNIR is to convert data from detector counts in the instrument geometry to reciprocal space, and to visualise the data in 1, 2, and 3 dimensions. The software also possesses tools to predict specific instrument configurations which are used for planning purposes and can mask spurious features both in the planing and visualisation steps, guiding users to

understand their measurements more easily. In this section, three of these main features are presented in more detail. These are the scan prediction tool, the 3D visualisation of data, and the masking framework.

The aim of the prediction tool is to find the optimal configuration of the instrument and the sample rotation scans needed for a spe-

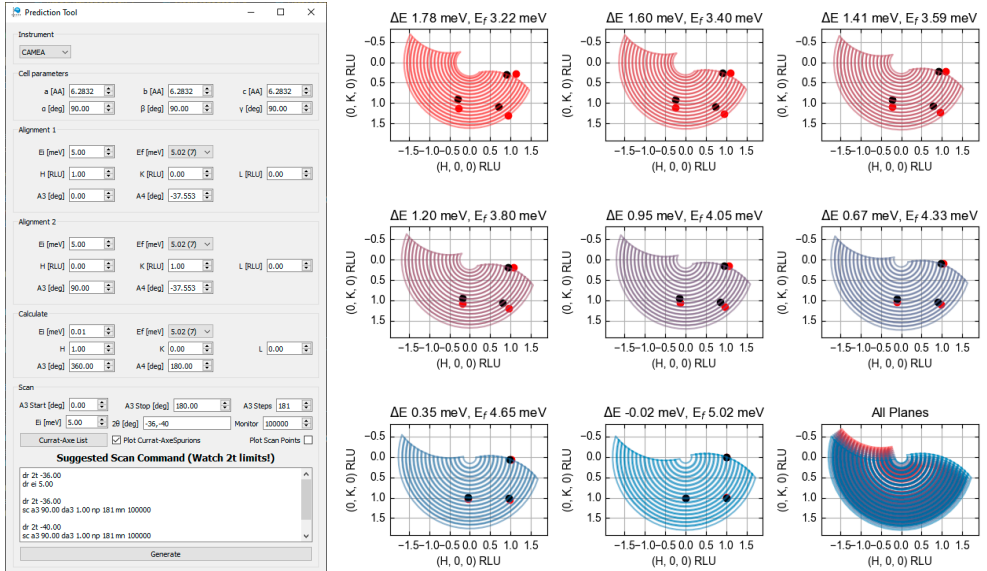


**Figure 3**

**Left:** Prediction tool for a cubic sample with  $a = 2\pi$ ,  $E_i = 5.0$  meV and two scattering angle settings ( $-36^\circ$  and  $-40^\circ$ ). **Right:** Plot of prediction  $180^\circ$  sample rotation scan for all 8 main energy transfers together with a combined coverage plot in the lower right panel. Each of the 8 individual plots also display the predicted positions for the Currat-Axe spurions for Bragg peaks  $(1, 0, 0)$ ,  $(1, 1, 0)$ , and  $(0, 1, 0)$ .

cific coverage in  $(\vec{Q}, E)$  space. For this, the sample of interest needs to be described in terms of its unit cell parameters and orientation with respect to the scattering plane of the instrument. In MJOLNIR, the sample and scattering plane is implemented via a TAS UB library that is converted from the PSI instrument control system. The library calculates corresponding scattering angles and sample rotation offsets of all crystal types and scattering planes through a UB matrix. By choosing a multiplexing instrument, its incoming energy, scattering angles, and sample rotation scan range, the prediction tool calcu-

lates the covered part in reciprocal space and shows it for each analyser unit. The covered range is plotted in reciprocal lattice units RLU in units of  $1/\text{\AA}$ , which are overlaid with the relevant crystal reciprocal lattice reflecting the scattering plane and lattice parameters, see Fig. 3.

The plotting method makes use of advanced features in the Python plotting library Matplotlib<sup>12</sup> and is also used to generate an interactive visualisation of acquired data in multiple dimensions. Using View3D, the data files are binned into user-specified equi-sized voxels, which allows the user to

step through the data layer by layer at constant energy transfer or along two main directions. This gives a quick view into the data, allows the user to gauge the statistical significance of features, and aids during the experiment and in the initial data analysis phase.

Masking has been fully implemented in the upcoming releases of MJOLNIR (1.1.24) and MJOLNIRGui (0.9.9). The tool enables masking of various ranges of one or more parameters, e.g. an area in reciprocal space or a CurratAxe Spurion<sup>1</sup>, potentially simultaneous. These masks follow Boolean algebra and one can thus chain different masks together either as logical or or with logical and operators. The masks have been written in such a way that they are independent from the data files upon which they are applied and can thus be used across different data sets and instruments.

alongside MultiFLEXX at MIRA, which are both located at MLZ FRM2. It also serves as a path finder for the software needed at the up-coming BIFROST instrument at the European Spallation Source where an even higher data complexity is to be dealt with. MJOLNIR is expected to enable cutting edge research within the condensed matter community removing the need for users to be experts in the multiplexing instrument for then instead to focus on the science measured by them.

## IV. Conclusion

The increasing complexity in multiplexing spectrometers ranging from RITA-II over Flat-Cone to MultiFLEXX and CAMEA has lead to new software challenges in the post-processing of inelastic neutron scattering data. The MJOLNIR software package allows to convert, visualise, and analyse neutron scattering data stemming from multiplexing triple axis instruments. The software is also used during the planning of experiments in deciding the specific scans prior performed during the experiment, and has the potential to become the standard software for all multiplexing TAS instruments. MJOLNIR is currently in full operation at CAMEA at PSI and is planned to be used at the BAMBUS spectrometer of Panda,

- <sup>1</sup> G. Shirane, S. M. Shapiro, and J. M. Tranquada, *Neutron Scattering with a Triple-Axis Spectrometer* (Cambridge, 2004).
- <sup>2</sup> K. Lefmann, D. F. McMorrow, H. M. Rønnow, K. Nielsen, K. N. Clausen, B. Lake, and G. Aeppli, *Physica B: Condensed Matter* **283**, 343 (2000).
- <sup>3</sup> W. Schmidt and M. Ohl, *Physica B: Condensed Matter* **385-386**, 1073 (2006).
- <sup>4</sup> J. Lass, C. R. Andersen, H. K. Leerberg, S. Birkemose, S. Toth, U. Stuhr, M. Bartkowiak, C. Niedermayer, Z. Lu, R. Toft-Petersen, M. Retuerto, J. O. Birk, and K. Lefmann, *Physical Review B* **101**, 54415 (2020), arXiv:1909.13734.
- <sup>5</sup> M. Kempa, B. Janousova, J. Saroun, P. Flores, M. Boehm, F. Demmel, and J. Kulda, *Physica B: Condensed Matter* **385**, 1080 (2006).
- <sup>6</sup> F. Groitl, R. Toft-Petersen, D. Quintero-Castro, S. Meng, Z. Lu, Z. Hüsches, M. D. Le, S. Alimov, T. Wilpert, K. Kiefer, S. Gerischer, A. Bertin, and K. Habicht, *Sci. Rep.* **7**, 13637 (2017).
- <sup>7</sup> J. Lass, D. G. Mazzone, H. Jacobsen, K. M. Krighaar, D. Graf, F. Groitl, C. Kägi, R. Müller, R. Bürge, M. Schild, M. S. Lehmann, A. Bollhalder, P. Keller, M. Bartkowiak, U. Filges, F. Herzog, U. Greuter, G. Theidel, H. M. Rønnow, and C. Niedermayer, arXiv, 1 (2020), arXiv:2007.14796.
- <sup>8</sup> J. O. Birk, M. Markó, P. G. Freeman, J. Jacobsen, R. L. Hansen, N. B. Christensen, C. Niedermayer, M. Månsson, H. M. Rønnow, and K. Lefmann, *Review of Scientific Instruments* **85** (2014), 10.1063/1.4901160, 1408.0551.
- <sup>9</sup> J. Lass, H. Jacobsen, D. G. Mazzone, and K. Lefmann, *SoftwareX* **12**, 100600 (2020).
- <sup>10</sup> G. Van Rossum and F. L. Drake, *Python 3 Reference Manual* (CreateSpace, Scotts Valley, CA, 2009).
- <sup>11</sup> J. Lass, M. E. Bøggild, P. Hedegård, and K. Lefmann, *Journal of Neutron Research* **1**, 1 (2020), arXiv:2006.03812.
- <sup>12</sup> J. D. Hunter, *Computing in Science & Engineering* **9**, 90 (2007).

# Measurement of liquids surface tension in extreme environments using neutron imaging

Ondřej Vopička <sup>1,\*</sup>, Petr Číhal <sup>1</sup>,  
Martina Klepič <sup>1</sup>, Jan Crha <sup>2</sup>, Vladimír Hynek <sup>1,3</sup>,  
Karel Trtík <sup>3</sup>, Pierre Boillat <sup>2</sup>, Pavel Trtik <sup>2,\*\*</sup>

<sup>1</sup> Department of Physical Chemistry, University of Chemistry and Technology, Prague, Technická 5, 166 28 Prague 6, Czech Republic

<sup>2</sup> Laboratory for Neutron Scattering and Imaging, Paul Scherrer Institut, Forschungsstrasse 111, CH-5232 Villigen, Switzerland

<sup>3</sup> Universita třetího věku (U3V), Czech Technical University in Prague, Thákurova 7, 166 29 Prague 6, Czech Republic

\* Corresponding author:  
ondrej.vopicka@vscht.cz

\*\* Corresponding author: pavel.trtik@psi.ch

## Abstract

We report a powerful method for the assessment of surface tension of liquids exposed to highly pressurized gas. The method is based on high resolution neutron imaging (pixel size  $\sim 21 \mu\text{m}$ ) and utilizes the axial symmetry of the high-pressure experimental cells for the tomographic reconstructions of the profiles of the liquid menisci. Based on these profiles, contact angle and surface tension are evaluated using the Young-Laplace equation. In the proof-of-principle investigation, the surface tension of deuterated ethanol ( $\text{C}_2\text{D}_6\text{O}$ ) and deuterated *n*-decane ( $n\text{-C}_{10}\text{D}_{22}$ ) under high pressure of methane ( $\text{CH}_4$ ) were investigated at two temperatures and two pressures of methane, namely 7.0, 37.8 °C and 80, 120 bar. The aforementioned surface characteristics of ethanol, a methane hydrate inhibitor, and *n*-decane, a model constituent of crude oil, were thus measured in non-tactile manner under industrially relevant conditions.

## Introduction

Methane has been forecast to become the second most used energy resource within the

next two decades [1]. The production of this gas, which can be seen as a bridge to low-carbon energy future [2], is inherently related to its basic properties, such as its ability to absorb and diffuse in liquids. Methane absorption naturally influences the properties of the liquid, such as density and surface tension. Ethanol is an industrially relevant inhibitor of the methane hydrate formation [3]. *n*-decane is a model constituent of crude oil. Information on their surface tension and contact angle characteristics under high pressures are crucial for the production, refining and transportation of the natural gas and crude oil, such as for the enhanced oil recovery by conducting pressurized gases to oil wells [4].

The surface tension and contact angle under high pressures can be measured, to our knowledge, using the pendant drop method [5], methods based on capillary waves [6] or capillary rise [7]. These methods are either tactile or typically utilise visible light for the detection. Literature data on surface tension and related characteristics, such as liquid density and gas solubility, are available either for *n*-decane and methane or for similar systems under high pressures [6],[8],[9],[10].

Neutron imaging possesses a high potential for investigations of liquids under high pressures in opaque vessels. When compared to other radiations and fields, neutrons allow for the highly spatially resolved radiography [11], and show high penetrability through metals. This allows highly mechanically stable and simultaneously rather transparent measuring cells to be constructed for in-situ neutron imaging experiments. To our knowledge, neutron imaging has not been

previously used to study the surface phenomena at high pressures. In order to increase the contrast between the liquid and (dissolved) gas, the large difference in the neutron cross-section of protium (H) and deuterium (D) can be well utilized. Although density of a liquid naturally depends on the isotopic composition of the compound, its molar volume does not vary significantly [12],[13]. Besides that, surface tensions of liquids show minor dependences on their isotopic compositions [14] for a series of perdeuterated and perprotonated (normal) C<sub>6</sub>-C<sub>8</sub> alkanes and aromatic compounds; the differences in the surface tensions of these liquids ranged 0.5–0.8 mN·m<sup>-1</sup> or less, that is, approximately, 5% or less. Thus, as limited differences of the physical properties occur due to the interchange of protium and deuterium in the studied molecules, the results presented here are relevant not only for the deuterated but also for the protonated “normal” chemicals.

Based on the Young-Laplace equation, the shape of the liquid-gas (also liquid-supercritical fluid) interface in a tube of axial symmetry and non-negligible diameter in gravitational field follows [15],[16] the differential equation

$$z = \frac{\gamma}{\Delta\rho \cdot g} \cdot \left( \frac{z''}{1 + z'^2} + \frac{z'}{y(1 + z'^2)^{1/2}} \right) \quad (1)$$

in which  $z$  is the meniscus profile,  $y \in (0, r)$  spatial coordinate,  $r$  inner diameter of the tube,  $\Delta\rho$  is the difference of the densities of the liquid and gaseous (supercritical fluid) phases,  $g = 9.80740 \text{ m}\cdot\text{s}^{-2}$  is gravity,  $\gamma$  is surface tension. As Eq. (1) can be numerically solved under conditions  $z'(y = 0) = 0$  and  $z'(y = r) = \cot \theta$ , three adjustable para-

meters (contact angle  $\theta$ , surface tension, position of the meniscus) can be calculated by fitting the calculated profiles to the experimental menisci shapes.

The dependence of the surface tension on pressure in a binary system methane-liquid follows [26]

$$\left(\frac{\partial\gamma}{\partial p}\right)_{\text{Area},T} = -c_A^S \frac{(1 - x_A^{\text{liq.}})\bar{V}^{\text{gas}} - (1 - x_A^{\text{gas}})\bar{V}^{\text{liq.}}}{x_A^{\text{gas}} - x_A^{\text{liq.}}} \cong -c_A^S \bar{V}^{\text{gas}} \quad (2)$$

in which  $c_A^S$  stands for the surface excess concentration of methane. Following the convention taken from the literature, it is assumed that  $\bar{V}^{\text{gas}}$  can be approximated by the molar volume of (pure) methane and the methane phase is denoted as “gas” since the same formula can be used for the case of the supercritical fluid [17]; the right-hand side approximation holds for the systems at moderate pressures and negligible evaporation of the liquid. Specifically, following inequalities justify well that approximation for partial pressures of methane relevant to this work:  $x_{\text{C}_2\text{H}_6\text{O}}^{\text{gas}} < 0.004$  at 0 °C [18] and  $x_{\text{C}_2\text{H}_6\text{O}}^{\text{gas}} < 0.005$  at 40 °C [19] and  $x_{\text{C}_{10}\text{H}_{22}}^{\text{gas}} < 0.0014$  at 37.8 °C [20] and  $x_{n\text{-C}_8\text{H}_{18}}^{\text{gas}} < 0.003$  below 50 °C [21].

The surface excess concentration of methane thus yields [17]

$$c_A^S = -\frac{p}{zRT} \left(\frac{\partial\gamma}{\partial p}\right)_{\text{Area},T} \quad (3)$$

in which  $z$  is the gas compressibility factor.

The experiments reported here were conducted with supercritical methane. However, density and diffusivity of methane [9], surface tension of the liquid exposed to methane [17] and equilibrium solubility

[18],[19],[20],[21] of methane in liquids do not qualitatively change if pressure exceeds the critical pressure of methane within the conditions relevant to this work. The main reason for the use of supercritical methane ( $p > p_c$ ,  $T > T_c$ ) in this work was its higher density and, thus, higher neutron contrast when

compared to methane gas ( $p < p_c$ ,  $T > T_c$ ). Above that, the supercritical

conditions are also more relevant to the mentioned practical applications.

## Experimental setup and procedure

An apparatus that allowed for observation of two vessels with still liquids under the controlled external gas pressure and under controlled temperature was tailor-made for the purpose of this experiment. The apparatus consisted of two Titanium Grade 5 measuring cells placed in a duralmin body maintained at a constant temperature (Fig. 1); the whole apparatus was placed in a 2 mm thick duralmin safety box continuously purged with nitrogen to avoid vapour condensation. Deuterated ethanol ( $\text{C}_2\text{D}_6\text{O}$ ) was placed in one measuring cell (a cylinder with the centred  $9.0 \pm 0.1$  mm flat-bottomed bore and wall thickness 1.5 mm), deuterated  $n$ -decane ( $n\text{-C}_{10}\text{D}_{22}$ ) in the other one; the typical liquid level in each cell was about 1 – 1.5 cm. The liquids were then separately bubbled for ~1minute with nitrogen at a flow rate of ~20  $\text{cm}^3 \text{min}^{-1}$  using a stainless steel capillary connected to pressurized nitrogen temporarily submerged into the liquid. Afterwards, each

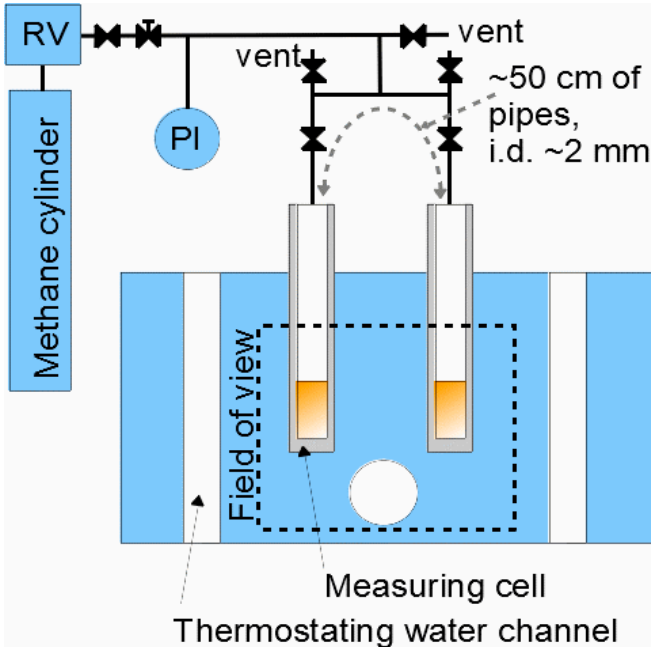


**Figure 1**

Scheme of the measuring apparatus. RV abbreviates reduction valve, PI pressure gauge with indication.

liquid was bubbled for  $\sim 1$  minute with methane at a flow rate of  $\sim 20 \text{ cm}^3 \text{ min}^{-1}$  and the whole apparatus was purged with methane to remove other gases. The apparatus containing the liquid equilibrated with methane at atmospheric pressure was then gradually charged with the compressed methane; each pressure change took 15-30 seconds. During the experiments, the two cells remained connected to the reduction valve to assure constant pressure. These cells were thus connected, during the experiments, with approx. 50 cm of tubing having the inner diameter of approx. 2 mm, which effectively avoided potential contamination of the gaseous phases by free diffusion. After the experiment, each cell and the surrounding tubing was separately opened to the atmosphere and purged with the pure methane.

The experiments were performed at the measuring position no. 2 of the NEUTRA thermal neutron beamline at Swiss spallation neutron source (SINQ) [22]. Further details of the experimental procedure and used materials can be found in Vopicka et al. [23].

A series of experiments on methane ( $\text{CH}_4$ ) absorption into still liquid bodies of deuterated ethanol ( $\text{C}_2\text{D}_6\text{O}$ ) and *n*-decane ( $n\text{-C}_{10}\text{D}_{22}$ ) was conducted at  $(7.0 \pm 0.5)^\circ\text{C}$  and at  $(37.8 \pm 0.5)^\circ\text{C}$ . These experiments were made in such a way that methane pressure was stepwise elevated from atmospheric pressure to approx. 80 bar and then to approx. 120 bar. Neutron radiographies were then acquired (see Fig. 2) to follow diffusion and change in the level of the liquids (swelling). In the case of the experiments at  $(7.0 \pm 0.5)^\circ\text{C}$ , methane pressure was stepwise changed

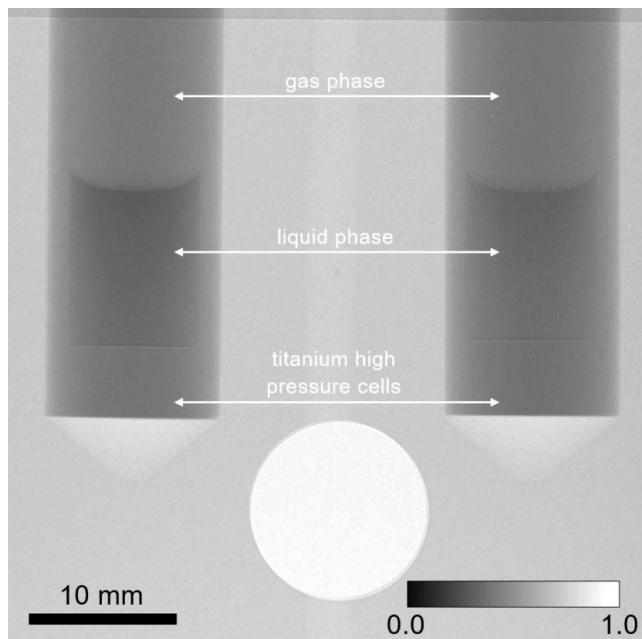


**Figure 2**

Neutron image of the setup after being pressurized with  $\text{CH}_4$  from 1.0 to 81.4 bar at 7.0 °C. Left cell:  $n\text{-C}_{10}\text{D}_{22}$ , right cell:  $\text{C}_2\text{D}_6\text{O}$ . Inner diameter of the measuring cell was  $9.0 \pm 0.1$  mm, outer 12 mm, grey intensity corresponds to transmittance.

from atmospheric pressure to approx. 120 bar for comparison.

The meniscus shape was evaluated for neutron radiographies collected for the state closest to the methane absorption equilibrium, that is, at the longest equilibration time at which neutron radiographies were taken. Although true equilibrium was not reached, the concentration gradient near the phase interface was rather small at long times and we thus assume that this did not significantly disturb the methane adsorption on the interface.

## Results

Based on the knowledge that the sample is axially symmetric, the transmittance image

measured by neutron radiography was converted to a tomographic slice using a method based on the onion peeling algorithm [24], in which the full geometrical description of the forward projection was used instead of its linear approximation. While the neutron radiographies are sufficient for the assessment of the concentration profile in the bulk liquid and its level, the thus-obtained tomographic slices (Fig. 3) are superior for the fitting of the model to the actual meniscus profile. Naturally, the linear attenuation coefficient of the methane phase as well as of the liquid phase increased with the methane pressure. The titanium high-pressure cell served here as a convenient reference material. The observed cross-section of Titanium Grade 5 (having the average mole-based ratios of the main constituents  $\text{Ti}:\text{Al}:\text{V} =$

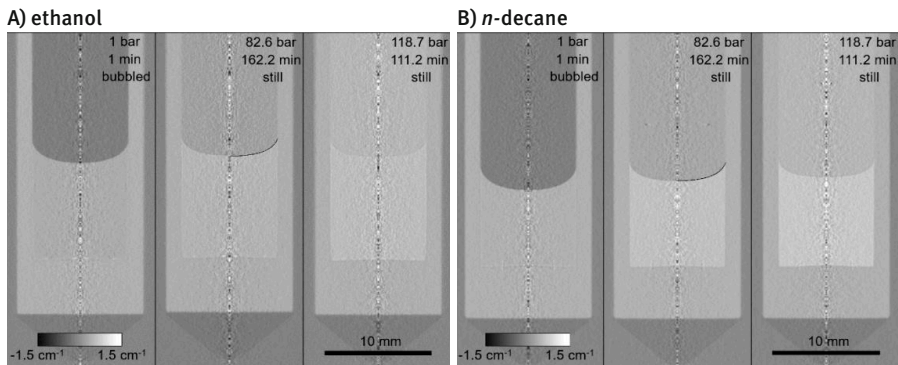


**Figure 3**

Tomographic reconstructions of the titanium high pressure cell with the liquid body and methane phase for 1 bar (left), 82.6 bar (middle) and 118.7 bar (right) in each triad of the reconstructions. The model of the meniscus, solution of Eq. (1), is depicted as the black curve (at 82.6 bar, right half of the meniscus). Systems of  $C_2D_6O$  (A) and  $n-C_{10}D_{22}$  (B) with  $CH_4$  at 37.8 °C are shown, grey intensity corresponds to the linear attenuation coefficient,  $\Sigma$ . The inner diameter of each measuring cell is  $9.0 \pm 0.1$  mm.

0.859:0.105:0.036) is  $\sigma_{TiG5} = (10.2 \pm 0.9)$  barn, i.e.  $\Sigma_{TiG5} = (0.57 \pm 0.05) \text{ cm}^{-1}$ , while the theoretical estimate for the alloy of this composition from NIST is  $\Sigma_{TiG5} = 0.558 \text{ cm}^{-1}$ . The shape of the meniscus was approximated with the numerical solution of Eq. (1), in which the parameters were calculated fitting the model to the experimental profile (Fig. 3 and Table 1). Density difference, a parameter of Eq. (1), was calculated based on  $\rho^D$  averaged for the all types of evaluation (for details see Table 2 in [23]), and on the state behaviour of pure methane as described with the Peng-Robinson equation of state [25]. The evaporation of ethanol and  $n$ -decane into methane was neglected; see comments below Eq. (2). The expected uncertainties of  $\theta$  ( $\pm 2^\circ$ ) and  $\gamma$  ( $\pm 2 \text{ mN}\cdot\text{m}^{-1}$ ) were estimated as the propagated uncertainties of how the numerical solution of Eq. (1) fits the tomo-

graphic reconstructions of the menisci, the uncertainty of the diameter of the measuring cell and of the density difference. No influence of the mode of the pressurization (single step and two consecutive steps) or of the initial liquid level (approximately 1 cm and 1.5 cm, both at 7.0 °C) on the measured quantities was discerned, thereby again indicating good consistency of the method.

Contact angle was found to be independent of temperature and methane pressure for both studied compounds within the inspected conditions and within the experimental uncertainty. Surface tensions of pure perdeuterated ethanol and  $n$ -decane (neglecting dissolution of methane at 1.0 bar) were consistent with the available literature data (Table 1) and showed an expectable temperature dependence. The dependence of the surface tension on the methane pres-

Methane (CH <sub>4</sub> ) and ethanol (C <sub>2</sub> D <sub>6</sub> O)				
Temperature, °C	Pressure of CH <sub>4</sub> , bar	γ, mN·m <sup>-1</sup>	θ, °	Equilibration time, conditions
7.0	1.0	22, 24*	15	1 min, bubbled before exp.
7.0	81.4 (1.0→81.4)	15	14	244.2 min, still
7.0	117.7 (81.4→117.7)	12	14	170.2 min, still
7.0	1.0	22, 24*	15	1 min, bubbled before exp.
7.0	118.7 (1.0→118.7)	12	13	363.2 min, still
37.8	1.0	21, 21*	16	1 min, bubbled before exp.
37.8	82.6 (1.0→82.6)	14	14	162.2 min, still
37.8	118.7 (82.6→118.7)	11	13	111.2 min, still
Methane (CH <sub>4</sub> ) and <i>n</i> -decane ( <i>n</i> -C <sub>10</sub> D <sub>22</sub> )				
Temperature, °C	Pressure of CH <sub>4</sub> , bar	γ, mN·m <sup>-1</sup>	θ, °	Equilibration time, conditions
7.0	1.0	25, 25.1*	9	1 min, bubbled before exp.
7.0	81.4 (1.0→81.4)	15	8	244.2 min, still
7.0	117.7 (81.4→117.7)	11	10	170.2 min, still
7.0	1.0	25, 25.1*	8	1 min, bubbled before exp.
7.0	118.7 (1.0→118.7)	10	10	363.2 min, still
37.8	1.0	22, 22.2*	8	1 min, bubbled before exp.
37.8	82.6 (1.0→82.6)	13	12	162.2 min, still
37.8	118.7 (82.6→118.7)	10	11	111.2 min, still

\* Data from the database [26] for ethanol (C<sub>2</sub>H<sub>6</sub>O) and *n*-decane (*n*-C<sub>10</sub>H<sub>22</sub>).

**Table 1**

Surface tension and contact angle of deuterated ethanol (C<sub>2</sub>D<sub>6</sub>O) and deuterated *n*-decane (*n*-C<sub>10</sub>D<sub>22</sub>) saturated with methane (CH<sub>4</sub>) at given pressures and temperatures.

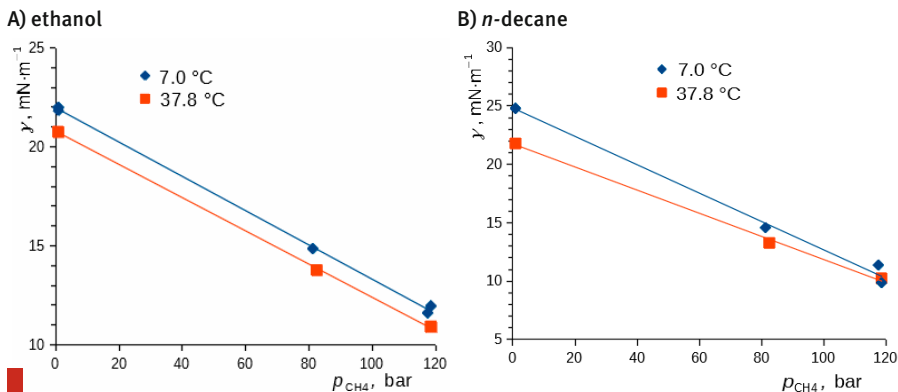


**Figure 4**

Surface tension of solutions of  $\text{CH}_4$  in  $\text{C}_2\text{D}_6\text{O}$  (A) and in  $n\text{-C}_{10}\text{D}_{22}$  (B) as functions of methane ( $\text{CH}_4$ ) pressure. Linear fits calculated using the least squares method are shown.

sure was well parameterized with the approximate form of Eq. (2), see Fig. 4.

The pressure derivatives of the surface tension yielded:

$$(\partial\gamma/\partial p)_{\text{Area},7.0\text{ }^\circ\text{C}} = -0.87 \text{ nm}$$

$$(\partial\gamma/\partial p)_{\text{Area},37.8\text{ }^\circ\text{C}} = -0.84 \text{ nm}$$

$$\text{and } (\partial\gamma/\partial p)_{\text{Area},7.0\text{ }^\circ\text{C}} = -1.22 \text{ nm}$$

$$\text{and } (\partial\gamma/\partial p)_{\text{Area},37.8\text{ }^\circ\text{C}} = -0.99 \text{ nm}$$

for *n*-decane, respectively. The latter compares well with the value of around  $-1.3 \text{ nm}$  as calculated from the data reported for *n*-hexane and methane at  $25\text{ }^\circ\text{C}$  observed using the capillary rise method [7], for which the authors admitted that equilibrium was probably not reached, or  $-0.88 \text{ nm}$  reported for heptane in argon at  $288 \text{ K}$  as determined using the measurement of capillary waves [6]. Interestingly, the above derivatives are comparable to those reported in the literature [25, 26, 30] for water and methane ( $-1.3 \text{ nm}$ ) despite the much lower methane solubility. The surface excess concentrations of methane on the surface of ethanol at  $120 \text{ bar}$  were  $c_{\text{A},7.0\text{ }^\circ\text{C}}^{\text{S}} = 5.8 \cdot 10^{-6} \text{ mol}\cdot\text{m}^{-2}$  and

$c_{\text{A},37.8\text{ }^\circ\text{C}}^{\text{S}} = 4.6 \cdot 10^{-6} \text{ mol}\cdot\text{m}^{-2}$ , while the same quantity for *n*-decane yielded  $c_{\text{A},7.0\text{ }^\circ\text{C}}^{\text{S}} = 8.2 \cdot 10^{-6} \text{ mol}\cdot\text{m}^{-2}$  and  $c_{\text{A},37.8\text{ }^\circ\text{C}}^{\text{S}} = 5.5 \cdot 10^{-6} \text{ mol}\cdot\text{m}^{-2}$ ; see Eq. (3). This compares well with the surface excess of  $(10 \pm 2) \cdot 10^{-6} \text{ mol}\cdot\text{m}^{-2}$  for the monolayer formed by spherically shaped methane molecules [17].

Overall, this pioneering investigation not only extends the limits of the available methods for assessment of surface tension and contact angle, but also serves as a validation of the applicability of the neutron imaging technique for the phenomena having known basic principles. Clearly, this method can contribute in future to the explanation of not well understood phenomena occurring under harsh conditions. We prospect this method to be used to follow the kinetics of the methane hydrate formation and decomposition, which remains not completely understood, in particular for still liquids. Moreover, we foresee to use the nontactile methodology for the assessment of the interfacial tensions

of supercooled liquids under high gas pressures as our method avoids triggering of solidification and enables its detection. All these surface phenomena have consequences not only for the production, refining and transportation of the natural gas and crude oil, but also for the understanding of the methane release from the methane hydrate beds to the atmosphere due to climate changes and contribute to the long studied but still not well understood behaviour of supercooled liquids.

## Conclusions

We report a new powerful method for investigation of the surface phenomena of liquids exposed to the high gas pressures. The method has been pilot tested for two still

liquids (ethanol,  $C_2D_6O$  and *n*-decane, *n*- $C_{10}D_{22}$ ) under high pressure of methane. The method, which is based on the neutron imaging of a cell containing a deuterated liquid upon its pressurization with a gas containing protium in its molecule, proved the ability to provide information on surface characteristics under industrially relevant conditions for the production and processing of crude oil and natural gas.

## Acknowledgements

This work is based on experiments performed at the Swiss spallation neutron source SINQ, Paul Scherrer Institute, Villigen, Switzerland, (beamtime proposal No. 20180283). The work presented in this short highlight is a part of a larger publication [23].

## REFERENCES

- [1] H.T. Lu, L. Liu, S. Kanehashi, C.A. Scholes, S.E. Kentish, The impact of toluene and xylene on the performance of cellulose triacetate membranes for natural gas sweetening, *J. Memb. Sci.* 555 (2018) 362–368. <https://doi.org/10.1016/j.memsci.2018.03.045>.
- [2] R.A. Kerr, Bursts Onto the Scene, *Sci. Mag.* 328. 328 (2010) 1624–1626.
- [3] E.D. Sloan, C.A. Koh, *Clathrate hydrates of natural gases*, third edition, 2007.
- [4] H.M. Sebastian, J.J. Simnick, H.M. Lin, K.C. Chao, Gas-liquid equilibrium in binary mixtures of methane with tetralin, diphenylmethane, and 1-methylnaphthalene, *J. Chem. Eng. Data.* 24 (1979) 149–152. <https://doi.org/10.1021/je60081a005>.
- [5] A.B. Chhetri, K.C. Watts, Surface tensions of petro-diesel, canola, jatropha and soapnut biodiesel fuels at elevated temperatures and pressures, *Fuel.* 104 (2013) 704–710. <https://doi.org/10.1016/j.fuel.2012.05.006>.
- [6] J. Dechoz, C. Rozé, Surface tension measurement of fuels and alkanes at high pressure under different atmospheres, *Appl. Surf. Sci.* 229 (2004) 175–182. <https://doi.org/10.1016/j.apsusc.2004.01.057>.
- [7] W.C. Slowinski E], Gates EE, The effect of pressure on the surface tensions of liquids, I (1956) 1948–1950.
- [8] H.H. Reamer, B.H. Sage, Diffusion coefficients in hydrocarbon systems: Methane in the liquid phase of the methane–*n*-heptane system, *AIChE J.* 3 (1957) 449–453. <https://doi.org/10.1002/aic.690030406>.
- [9] M. Jamialahmadi, M. Emadi, H. Müller-Steinhagen, Diffusion coefficients of methane in liquid hydrocarbons at high pressure and temperature, *J. Pet. Sci. Eng.* 53 (2006) 47– 60. <https://doi.org/10.1016/j.petrol.2006.01.011>.

- [10] S. Srivastan, N.A. Darwish, K.A.M. Gasem, R.L. Robinson, Solubility of Methane in Hexane, Decane, and Dodecane at Temperatures from 311 to 423 K and Pressures to 10.4 MPa, *J. Chem. Eng. Data.* 37 (1992) 516–520. <https://doi.org/10.1021/je00008a033>.
- [11] P. Trtik, E.H. Lehmann, Progress in High-resolution Neutron Imaging at the Paul Scherrer Institut-The Neutron Microscope Project, *J. Phys. Conf. Ser.* 746 (2016). <https://doi.org/10.1088/1742-6596/746/1/012004>.
- [12] P.G. Hill, R.D.C. Macmillan, V. Lee, A Fundamental Equation of State for Heavy Water, *J. Phys. Chem. Ref. Data.* 11 (1982) 1–14. <https://doi.org/10.1063/1.555661>.
- [13] I. Cibulka, T. Takagi, P- $\rho$ -T data of liquids: summarization and evaluation. 6. Nonaromatic hydrocarbons (C<sub>n</sub>, n  $\geq$  5) except n-alkanes C5 to C16, *J. Chem. Eng. Data.* 44 (1999) 1105–1128. <https://doi.org/10.1021/je990140s>.
- [14] D.G. LeGrand, G.L. Gaines, The polarizability of some deuterated hydrocarbons, *J. Phys. Chem.* 98 (1994) 4842–4844. <https://doi.org/10.1021/j100069a012>.
- [15] U. Henriksson, J.C. Eriksson, Thermodynamics of capillary rise: Why is the meniscus curved?, *J. Chem. Educ.* 81 (2004) 150–154. <https://doi.org/10.1021/ed081p150>.
- [16] A.W. Adamson, *Physical chemistry of surfaces*, 1997.
- [17] W. Sachs, V. Meyn, Pressure and temperature dependence of the surface tension in the system natural gas/water, *Colloids Surfaces A Physicochem. Eng. Asp.* 94 (1995) 291–301.
- [18] M.H. Kapateh, A. Chapoy, R. Burgass, B. Tohidi, Experimental Measurement and Modeling of the Solubility of Methane in Methanol and Ethanol, *J. Chem. Eng. Data.* 61 (2016) 666–673. <https://doi.org/10.1021/acs.jced.5b00793>.
- [19] K. Suzuki, H. Sue, M. Itou, R.L. Smith, H. Inomata, K. Arai, S. Saito, Isothermal Vapor- Liquid Equilibrium Data for Binary Systems at High Pressures: Carbon Dioxide- Methanol, Carbon Dioxide-Ethanol, Carbon Dioxide-1-Propanol, Methane-Ethanol, Methane-1-Propanol, Ethane-Ethanol, and Ethane-1-Propanol Systems, *J. Chem. Eng. Data.* 35 (1990) 63–66. <https://doi.org/10.1021/je00059a020>.
- [20] A.N. Reamer, H.H. Olds, R.H., Sage B.H. Lacey, Phase Equilibria in Hydrocarbon Systems, *Ind. Eng. Chem.* 34 (1942) 1526.
- [21] W. Kohn J.P., Brandish, Multiphase and Volumetric Equilibria of the Methane-n- Octane System at Temperatures between  $-110^{\circ}$  and  $150^{\circ}\text{C}$ ., *J. Chem. Eng. Data.* 9 (1964) 5.
- [22] B. Blau, K.N. Clausen, S. Gvasaliya, M. Janoschek, S. Janssen, L. Keller, B. Roessli, J. Schefer, P. Tregenna-Piggott, W. Wagner, W. Wagner, O. Zaharko, The Swiss Spallation Neutron Source SINQ at Paul Scherrer Institut, *Neutron News.* 20 (2009) 5–8. <https://doi.org/10.1080/10448630903120387>.
- [23] O. Vopička, P. Číhal, M. Klepič, J. Crha, V. Hynek, K. Trtík, P. Boillat, P. Trtik, One-pot neutron imaging of surface phenomena, swelling and diffusion during methane absorption in ethanol and n-decane under high pressure, *PLoS One.* 15 (2020) 1–24. <https://doi.org/10.1371/journal.pone.0238470>.
- [24] C.J. Dasch, One-dimensional tomography: a comparison of Abel, onion-peeling, and filtered backprojection methods, *Appl. Opt.* 31 (1992) 1146. <https://doi.org/10.1364/ao.31.001146>.
- [25] D. Peng, D.B. Robinson, A New Two-Constant Equation of State A New Two-Constant Equation of State, 15 (1976) 59–64.
- [26] DIPPR Project 801 - Full Version: Design Institute for Physical Property Research/AIChE; Available from: <https://app.knovel.com/hotlink/toc/id:kpDIPPRPF7/dippr-project-801-full/dippr-project-801-full,n.d>.

# Minutes of the SGN/SSSN/SNSS General Assembly 2021

## Date/Location

November 26, 2021, Paul Scherrer Institut

## Start

14:00

## End

17:00

## Participants

12 members of the society and  
5 non-members

## 1. Welcome

Henrik Rønnow, president of the Swiss Neutron Science Society, welcomes the participants to the general assembly 2021.

Before the assembly, scientific presentations by the two winners of the 2021 Young Scientist Prize of the SNSS sponsored by SwissNeutronics.

## 2. Minutes of the General Assembly 2020

The minutes of the general assembly of the SNSS/SGN from 29.10.2020, published in Swiss Neutron News #57 are accepted without objections.

## 3. Annual Report of the Chairman

Henrik Rønnow reports on the activities of the SNSS/SGN in the years 2019 and 2020:

- a. The eighth (2021) **Young Scientist Prize** of the SNSS/SGN sponsored by Swiss Neutronics has been split and was awarded to Dr. Jakob Lass and Dr. Jacopo Valsecchi. The deadline for nominations for the 2022 Young Scientist Prize is February 28, 2022.
- b. The SNSS/SGN has **204 members** at the time of the assembly. The number of members has increased by 1 compared to 2020.

The number of SNSS members is still significantly lower than that of neutron users in Switzerland. The number of unique Swiss proposers (with a Swiss email address) for beam time at SINQ from 2015 to 2020 was 419. The visibility of the SNSS should be improved for all neutron users, especially new users at SINQ.

- c. A new strategy paper for science using neutrons in Switzerland, the Neutron Science Roadmap, was published by SNSS in collaboration with the Swiss Academy Sciences. The Roadmap can be found on the SNSS web page: <https://sgn.web.psi.ch/sgn/strategy.html>. Next to contributions from the Swiss neutron community, the Roadmap is based on a bibliometrics

study of publications involving all areas of neutron science. It is found that the Swiss neutron science community is growing at a rate of about 5% per year and that the Swiss neutron community is remarkably diverse with branches to many science fields and industries. The Swiss neutron science community also produces 10% of neutron publications in Europe or 5% world-wide. This is remarkable considering that Switzerland only makes up about 2% of the European population.

- d. One issue of **Swiss Neutron News** has appeared in April 2021 and another issue was in print at the time of the assembly and was distributed at the end of November 2021.

#### 4. Report of the Treasurer

The annual balance sheet for 2020 is presented:

Note that the payout of CHF 2000.00 for the prize money is due to CHF 1000.00 prize money from the previous year remaining on the SNSS account until the beginning of 2020.

Assets SNSS/SGN on 1.1.2012:

**CHF 8303.30**

	Revenues [CHF]	Expenses [CHF]
Membership-fees (cash box)	0.00	
Membership-fees (postal check acc.)	920.00	
Donations	0.00	
Deposit prize money 2020	1000.00	
Expenses Postfinance account		61.50
Payout prize money 2020		2000.00
Total	1920.00	2061.50
Net earnings 2020	<b>CHF -141.50</b>	

Balance sheet 2020:	Assets [CHF]	Liabilities [CHF]
Postfinance account	7941.80	
Cash box	220.00	
<b>Assets on 31.12.2019</b>	<b>8161.80</b>	

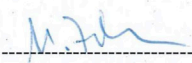
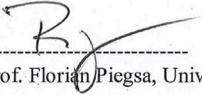
## 5. Report of the Auditors

Both Auditors (M. Zolliker and F. Piegsa) have examined the bookkeeping and the balance sheet for 2020. They have accepted it without

objection. The participants unanimously vote for the release of the SGN/SNSS board.

### Bericht der Revisoren

Die Rechnungsrevisoren haben die Belege, die Abrechnungen und die Bilanz für das Jahr 2020 geprüft und für in Ordnung befunden!

20.1.21		27.1.21	
Datum	Dr. M. Zolliker, PSI	Datum	Prof. Florian Piegsa, Univ. Bern

## 6. Budget 2020

H. Rønnow presents the following proposal for the budget 2022:

	Receipts [CHF]	Expenditures [CHF]
member fees	900.00	
interest	0.00	
prize money	1000.00	1000.00
fees PC account		63.00
Total	1900.00	1063.00
Total receipts 2022	837.00	
Assets 31.12.2022	8998.80	

The participants accept the budget proposal without objection.

## 7. Vote for a change of the SNSS by-laws

As the name of the society was changed to “Swiss Neutron Science Society” and the society was opened to more science fields using neutrons, the board proposes to increase the number of members of the board of SNSS from four to five.

For this, article 10 of the by-laws needs to be changed from “The executive committee consists of a president and a maximum of four other members.” to “The executive committee consists of a president and a maximum of five other members.”

This change of the by-laws is accepted unanimously.

## 8. Election of the SNSS board for the period 2022-2024

The board for the period 2019-2021 was Henrik Rønnow (president), Urs Gasser (board member and secretary), Karl Krämer (board member), and Markus Strobl (board member).

Henrik Rønnow steps down as president, and Marc Janoschek (University of Zurich / PSI) is proposed as new president. Henrik Rønnow is ready to remain available to the SNSS board. Urs Gasser steps down as secretary but is ready to remain available to the SNSS board. Karl Krämer and Markus Strobl are running again for the SNSS board. It is proposed that the duties of the secretary are distributed among the board members and Efthymios Polatidis (LNS, PSI) will take care of Swiss Neutron News. Further, it is proposed that Florian Piegsa (University of Bern,

auditor of SNSS) should join the board and that Henrik Rønnow should stay on the board.

Marc Janoschek is elected as the new president of SNSS with one abstention. Urs Gasser, Karl Krämer, and Markus Strobl are unanimously re-elected as board members. Florian Piegsa is elected as new board member without a dissenting vote. Henrik Rønnow is also elected as board member with one vote against.

The newly-elected president Marc Janoschek thanks everyone for the trust in him, and states that he is looking forward to this new tasks. He also thanks the former president Henrik Rønnow as well as the former secretary, Urs Gasser, for many years of service to the community since 2009. He also thanks Henrik to stay on the board for a transitional period and that he will be happy to hear his advice.

Henrik Rønnow thanks the Swiss neutron science community, the SNSS and the board for many exciting years. He states that the SNSS is really the work of the entire board and many colleagues throughout the community. The community is further thriving and visible world-wide. He wishes the new board, and the community the very best success going forward.

## 9. News from ENSA, ILL, and ESS

### 1) News from ILL (Henrik Rønnow)

- a. Paul Langdan is the new director of ILL, he has taken over on Oct. 1st 2021 from Helmut Schober.
- b. France, Germany, and the United Kingdom have prolonged their support for the ILL until 2033.

- c. The membership of Switzerland is secured until 2023 and is expected to be prolonged until 2028 with funding reduced from 15 MCHF to 12 MCHF per year.
  - d. In addition to the annual funding for the ILL, a budget for supplementary measures has been approved by SERI. Projects for the ILL that are also of interest for researchers using neutrons in Switzerland can be financed via the budget of the supplementary measures.
  - e. The Swiss participation in the CRG instruments IN12, IN22, and D23 operated by CEA helps to reduce the number of Swiss beam-time proposals being rejected due to national balance. Swiss users obtain beam time on these CRG instruments via the normal proposal system of the ILL. The Swiss participation in these CRG instruments has been extended to 2022 and may be continued further.
  - f. In recent years, the number of neutron beam cycles at ILL was reduced e.g. due to new safety regulations that had to be met.
  - g. Some countries are arrears with their payments to the ILL. Proposals with co-proposers from these countries have, therefore, not received beam time and the ILL is now strictly implementing the rule of national balance for the distribution of beam time. This is not in the interest of researchers from Switzerland.
  - h. In case your proposal is impeded by national balance, please send a short notice to the SNS (sgn@psi.ch) to make sure that the SNS can document the effect of the national balance.
- b. 81% of ESS are now complete. This entails that the civil construction (mostly buildings) is now basically completed. From November 10 to 15, 2021, ESS went through its second re-baselining review (the first was in 2018). The aim of this re-baselining is a realistic schedule with schedule and budget contingencies and resource loaded project schedule. A new plan with a ~80% probability for keeping the schedule has been proposed. For the ideal case of no further delays the important "beam on target" (BOT) milestone is projected to be in the fall of 2024. The schedule with 80% probability of reaching milestones includes more realistic schedule contingencies and projects BOT to be in 2026. At the time of BOT, the plan is to have 6/9 instruments in operation, and the rest in the hot commissioning phase. Stable operations are expected for 2028.
- c. Switzerland is a strong contributor to the ESS and is involved in five instruments for ESS: ESTIA, BIFROST, HEIMDAL, ODIN, and MAGIC. The instruments BIFROST, ESTIA (100% Swiss), ODIN and MAGIC are all scheduled to be among the first eight instruments to go into user-operation. ODIN even belongs to select group of the "first three" that are meant to show that ground-breaking science can be done at ESS early on. BIFROST, ESTIA and ODIN were all showcased by our project teams during the re-baselining review and were commended by the reviewers.

## II) News from ESS (Marc Janoschek)

- a. On November 1st, 2021, Helmut Schober has taken office as the new Director General of ESS.

## III) News from ENSA (Henrik Rønnow)

- a. Since Nov. 2019, Henrik Rønnow is the chair of ENSA. Lambert van Eijck (TU Delft) is the vice chair, and Natalie Malikova (CNRS, Paris) is the secretary of ENSA.

- b. The ICNS 2021 was postponed to 2022 and will be held in Buenos Aires, Argentina. The ECNS 2023 will take place in Munich, Germany.
- c. ENSA awards the Levy-Bertaut prize, the Walter-Hälg prize, and the prize for Neutron Innovation and Instrumentation. The calls for these prizes will be published soon.
- d. ENSA is a partner of the accepted European funding proposal BrightnESS2, a European-Union funded project to support the long-term sustainability of ESS, its community, and the network of neutron sources in Europe. Evgenii Velichko (TU Delft) has been employed by ENSA to analyze the neutron user community and its impact as well as to explore access models to ESS.
- e. Regular meetings of ENSA, NSSA, and AONSA have been initiated, and ENSA is collaborating with the League of advanced European Neutron Sources (LENS) and with ARIE, the network of high-level facilities that provide instruments and services to enable European researchers to address the Missions of Horizon Europe.

## 10. News from SINQ (Michel Kenzelmann)

- a. Although not all instruments are currently in the user program, a number of proposals has increased massively with 697 proposals for the first cycle of 2022. This has to be compared with 458 proposals for the user cycle in 2020, which was also a high number. The reasons for the increase include the recent closures of the neutron facilities HZB (Berlin, Germany), LLB (Saclay, France), and JEEP II (Kjeller, Norway), the problems at MLZ (Garching, Germany) with the cold neutron source, and the ILL shutdown in 2022. It is expected that the increased demand will persist at least until 2023.
- b. The number of publications has slightly decreased in 2020, this may be an effect caused by the shutdown in 2019.
- c. Several institutional agreements between PSI and other facilities have been reached in 2020 and 2021: The Norwegian institute for energy research, IFE, is investing 2.5 M€ in diffraction and imaging beam lines, and a Norwegian postdoc position at SINQ has been created. The decommissioned instrument SANS-II will be transferred to a new neutron facility in Argentina, which is financing software development projects together with SINQ. The SANS instrument PA20 from the LLB has been transferred to SINQ and will be available for both French and Swiss users under the new name SANS-LLB. This instrument is planned to be ready for users in the second half of 2022. The collaboration contract with DANSCATT for the common operation of neutron instruments has been renewed. The Laue diffractometer Falcon from HZB (Berlin) has been brought to SINQ and will be installed in 2022-2024.
- d. The Guide and Instrument Upgrade of SINQ in the years 2019 and 2020 has brought the expected gains in flux. The new spectrometer CAMEA has brought significant advantages for survey studies of a wider range in reciprocal space and also advantages for studies with small samples. Further, the new AMOR reflectometer can offer gains of a factor of ten or larger for small samples (commissioning in 2022). The new detector of the DMC diffractometer covers a much larger range in reciprocal space and allows for stu-

- dies of smaller samples (commissioning in 2022). The strongly over-booked SANS-I will be somewhat relieved by SANS-LLB as soon as it is commissioned. The imaging beam line Neutra and the diffractometer POLDI are planned to obtain upgrades during the shut-downs in 2022, 2023, and 2024 but should stay in the user program.
- e. The number of beam days sold to industry could be further increased with the help of ANAXAM, which acts as the link between the facilities of PSI and industry.
  - f. Within the Laboratory for Neutron Scattering and Imaging (LNS), the groups for applied materials and for soft matter will be strengthened. For soft matter, there will be strong link to the French community centered on the SANS-LLB instrument.
  - g. A preliminary study for a new North Guide Hall of SINQ has been started (2022-2025).

This could allow to install about 6 more instruments at SINQ and increase European neutron capacity for a relatively modest investment since there would be no extra costs running the neutron source SINQ.

- h. Collaborations with ESS during the operations phase of ESS will be explored. This will focus on the commissioning and the operation of instruments, and also on data analysis.

## 11. Miscellaneous

It is proposed to have SNSS assemblies via zoom to reach more members of the society.

U. Gasser  
December 2021

# Announcements

## SGN/SNSS Members

Presently the SGN/SNSS has 203 members. New members can register online on the SGN/SNSS website: <http://sgn.web.psi.ch>

## SGN/SSSN Annual Member Fee

The SGN/SNSS members are kindly asked to pay their annual member fees. At the general assembly 2013 of the society, the fee has been increased from CHF 10 to **CHF 20**. It can be paid either by bank transfer or in cash during your next visit at PSI. The bank account of the society is accessible for both Swiss national and international bank transfers: Postfinance: 50-70723-6 (BIC: POFICHBE), IBAN: CH39 0900 0000 5007 0723 6.

The SGN/SSSN is an organisation with tax charitable status. All fees and donations paid to the SGN/SSSN are **tax deductible**.

## PSI Facility News

Recent news and scientific highlights of the three major PSI user facilities SLS, SINQ and SpS can be found in the **quarterly electronic newsletter** available online under: <https://www.psi.ch/science/facility-news-letter>

## News from SINQ

DMC is currently being upgraded and equipped with a new high-performance 2D position-sensitive detector. The installation work successfully entered the hot commissioning phase. DMC will return to the SINQ user program later in 2022.

The reflectometer AMOR is undergoing a major upgrade and thereafter the respective commissioning phase. The instrument might be available for friendly users in late 2022.

In collaboration with the Laboratoire Léon-Brillouin (Saclay, France) the instrument SANS-LLB is being installed at SINQ. Commis-

sioning is planned for the first cycle in 2022, and SANS-LLB is planned to join the user program in the second cycle of 2022.

Recently, the users have been informed about the results of the proposal review for SINQ cycle I-22 (period May-August 2022). The next proposal submission deadline is planned for May 15, 2022 (beamtime period September-December 2022).

Please visit the page <https://www.psi.ch/sinq/call-for-proposals> to obtain the latest information about beam cycles and the availability of the neutron instruments.

## Registration of publications

Please remember to **register all publications either based on data taken at SINQ, SLS, SμS or having a PSI co-author** to the Digital Object Repository at PSI (DORA):

[www.dora.lib4ri.ch/psi/](http://www.dora.lib4ri.ch/psi/)

Please follow the link 'Add Publication'.

## Open Positions at SINQ and ILL

To look for open positions at SINQ or ILL, have a look at the following webpages:

<https://www.psi.ch/pa/stellenangebote>

<https://www.ill.eu/careers/all-our-vacancies/?L=0>

## PhD positions at ILL

The PhD program of the Institut Laue-Langevin, ILL, is open to researchers in Switzerland. Consult the page:

<https://www.ill.eu/careers/all-our-vacancies/phd-recruitment>

for information on the PhD program of ILL or get in contact with the managers of the program using the email address [phd@ill.fr](mailto:phd@ill.fr).

The Swiss agreement with the ILL includes that ILL funds and hosts one PhD student from Switzerland.

# Conferences and Workshops 2022 and beyond



An updated list with online links can be found here:  
<http://www.psi.ch/useroffice/conference-calendar>

## May 2022

CAROTS 2.0 STARTUP SCHOOL,

May - October 2022

May - October, 2022, online

FEBS 2022 Advanced Course

May 9-15, 2022, Spetses Island, Greece

LEAPS meets Quantum Technology  
Conference

May 15-20, 2022, Isola d'Elba, Italy

Swedish Neutron Week 2022

May 16-18, 2022, Norrköping, Sweden

International Operando Battery Days

May 16-18, 2022, Grenoble, France

Neutrons and Food 6

May 16-19, 2022, online

Foam-Scatter workshop

May 17, 2022, Grenoble, France

The extraordinary structure of ordinary  
things - A tribute to Isabelle Grillo

May 18-20, 2022, Grenoble, France

QENS/WINS 2022

May 23-27, 2022, San Sebastian, Spain

MLZ Conference 2022: Neutrons for mobility

May 31 - June 3, 2022, Lenggries, Germany

EPDIC17: Magnetic Structures and Neutron  
Scattering

May 31 - June 3, 2022, Šibenik, Croatia

## June 2022

MUST2022: International Conference on  
Molecular Ultrafast Science and Technology

June 7-10, 2022, Grindelwald, Switzerland

Diffuse scattering: the crystallography of  
dynamics, defects, and disorder

June 8-11, 2022, Erice, Italy

## LOPS 2022

June 10-12, 2022, Ft. Lauderdale, Florida, USA

Training on Neutron Techniques Summer School: Neutron Diffraction & Structural Imaging

June 12-18, 2022, San Giovanni in Valle Aurina, Italy

BESS 2022: Lipid Bilayers at ESS

June 13-15, 2022, Lund, Sweden

The Zurich School of Crystallography 2022

June 19-30, 2022, Zurich, Switzerland

IMoH 2022: First International Meeting on Opportunities and Challenges for HICANS

June 20-22, 2022, Leila, Spain

EMBO Practical Course — Small angle neutron and x-ray scattering from biomacromolecules in solution

June 20-24, 2022, Grenoble, France

Bombannes Summer School 2022

June 20-28, 2022, Carcan-Maubuisson (Gironde), France

SPS Annual Meeting 2022

June 27-30, 2022, Fribourg, Switzerland

BSR14: 14th International conference on Biology and Synchrotron Radiation

28 June - 1 July, 2022, Lund, Sweden

## July 2022

SPS Satellite Event: Women in Physics Career Symposium

July 1, 2022, Fribourg, Switzerland

NX School: 24th annual National School on Neutron and X-ray Scattering

July 10-22, 2022, Argonne and Oak Ridge National Laboratories, IL and TN, USA

## August 2022

3rd PSI Condensed Matter Summer Camp 2022

August 8-12, 2022, Zuzo, Switzerland

RACIRI Summer School "Advanced materials Design at X-ray and Neutron Facilities"

August 14-22, 2022, Varberg, Sweden

Exploring liquid properties in confined geometry at CMD29

August 21-26, 2022, Manchester, UK

ICNS 2022: 12th International Conference on Neutron Scattering

August 21-25, 2022, Buenos Aires, Argentina

2022 MolQueST (Molecule Based Quantum Science and Technology) Conference

August 21-25, 2022, Fondazione Monte Verità, Ascona, Switzerland

15th International Conference on Muon Spin Rotation, Relaxation and Resonance

August 28 - September 2, 2022, Parma, Italy

## September 2022

ILL and ESRF International Summer Programme on Neutron and X-Ray Science for undergraduate students  
September 4-30, 2022, Grenoble, France

SNI2022: 5th Conference on Research with Synchrotron Radiation, Neutrons and Ion Beams at Large Facilities  
September 5-7, 2022, Berlin, Germany

17th Oxford School on Neutron Scattering  
September 5-15, 2022, St. Anne's College, University of Oxford, UK

24th JCMS Laboratory Course - Neutron Scattering 2022  
September 5-16, 2022, Jülich and Garching, Germany

Open Access Days 2022  
September 19-21, 2022, Bern, Switzerland

Diffusion Fundamentals IX  
September 21-24, 2022, Krakow, Poland

## October 2022

Third ESS and ILL European Users Meeting  
October 5-7, 2022, Lund, Sweden

PSI 2022: 6th Workshop on "Physics of fundamental Symmetries and Interactions"  
October 16-21, 2022, PSI Villigen, Switzerland

Conférence internationale MATÉRIAUX 2022  
October 24-28, 2022, Lille, France

## March 2023

ECNS 2023: 8th European Conference on Neutron Scattering  
March 20-23, 2023, Garching, Germany





## Editorial

### Editor

Swiss Neutron Science Society

### Board for the Period 2022 – 2024:

#### President

Prof. Dr. M. Janoschek  
marc.janoschek@psi.ch

#### Board Members

PD Dr. U. Gasser  
urs.gasser@psi.ch

PD Dr. K. Krämer  
karl.kraemer@dcb.unibe.ch

Prof. Dr. F. Piegsa  
florian.piegsa@lhep.unibe.ch

Prof. Dr. H. Rønnow  
henrik.ronnow@epfl.ch

Prof. Dr. M. Strobl  
markus.strobl@psi.ch

### Honorary Members

Prof. Dr. W. Hälg, ETH Zürich (†)

Prof. Dr. K. A. Müller  
IBM Rüschlikon and Univ. Zürich

Prof. Dr. A. Furrer  
ETH Zürich and Paul Scherrer Institut

### Auditors

Dr. M. Zolliker, Paul Scherrer Institut  
Prof. Dr. F. Piegsa, Univ. Bern

### Address

Sekretariat SGN/SSSN/SNSS  
c/o Paul Scherrer Institut  
WLGA/018  
CH-5232 Villigen PSI  
phone: +41 56 310 46 66  
fax: +41 56 310 32 94  
<http://sgn.web.psi.ch>

### Bank Account

Postfinance: 50-70723-6 (BIC: POFICHBE)  
IBAN: CH39 0900 0000 5007 0723 6

### Printing

Paul Scherrer Institut  
Circulation: 1600  
2 numbers per year

### Copyright

SGN/SSSN/SNSS and the respective authors

### Swiss Neutron Science Society

Sekretariat SGN/SSSN/SNSS  
WLGA/018  
Paul Scherrer Institut  
5232 Villigen PSI, Switzerland



## **Join the Swiss Neutron Science Society...**

to support all science using neutron radiation in Switzerland.

The Swiss Neutron Science Society is open to everybody interested in neutron scattering and research using neutron radiation in general.

The annual membership fee is CHF 20.-, but the membership is free for Bachelor-, Master-, and PhD-students.

**Send an email to [sgn@psi.ch](mailto:sgn@psi.ch) to join.**